Second Kind Predictability of Climate Models

Peter C. Chu
Naval Ocean Analysis and Prediction Laboratory, Department of Oceanography
Naval Postgraduate School, Monterey, CA 93943, USA

Shihua Lu

Cold and Arid Regions Environmental and Engineering Research Institute
Chinese Academy of Sciences, Lanzhou, China

Abstract

Atmospheric and oceanic numerical models are usually initial-value and/or boundary-value problems. Change in either initial or boundary conditions leads to a variation of model solutions. Much of the predictability research has been done on the response of model behavior to an initial value perturbation. Less effort has been made on the response of model behavior to a boundary value perturbation. In this study, we use the latest version of the National Center for Atmospheric Research (NCAR) Community Climate Model (CCM3) to study the model uncertainty to tiny *SST* errors. The results show the urgency to investigate the second kind predictability problem for the climate models.

1. Introduction

Usually we use the Lorenz system (Lorenz, 1963)

$$\frac{dX}{d\tau} = -\sigma X + \sigma Y, \qquad (1)$$

$$\frac{dY}{d\tau} = -XZ + rX - Y, \qquad (2)$$

$$\frac{dZ}{d\tau} = XY - bZ, \qquad (3)^{1}$$

to illustrate the predictability due to the initial conditions X(τ_0), Y(τ_0), and Z(τ_0). This system was derived from the two-dimensional convection model consisting of a horizontal vorticity and heat equations. Here, X, Y, and Z are the first three terms in double Fourier series of stream function and temperature, τ is the dimensionless time, σ is the Prandtl number, b is the nondimensional parameter related to horizontal wavenumber, and r is the ratio between the Rayleigh number and its critical value and is proportional to the temperature difference between the lower and upper boundaries. Thus, the boundary condition error is represented by the error in r.

Recently, Chu (1999) found two kinds of predictability in the Lorenz system, namely, the model uncertainty due to the initial condition error (first kind) and due to the boundary condition error (second kind). The difference between the two is obvious. For the first kind predictability, the error is introduced only at the initial time instance ($\tau = \tau_0$). However, for the second kind of predictability, the error can be introduced at any time instance. To illustrate this, Chu (1999)

Corresponding Author: Professor Peter C. Chu, Naval Postgraduate School, Monterey, CA 93943, USA
Phone: 1-831-656-3688
E-mail: chu@nps.navy.mil

integrated (1)-(3) for three cases: a control run and two sensitivity runs. In the control run, he used the same initial conditions

$$X_c(0) = 0, \quad Y_c(0) = 1, \quad Z_c(0) = 0, \qquad (4)$$

and the same values for model parameters

$$r_c = 28, \quad \sigma_c = 10, \quad b_c = 8/3, \qquad (5)$$

as in Lorenz (1963). Here, the subscript *c* denotes the control run. In the two sensitivity runs everything was kept the same as the control run except the initial condition

$$Y_i(0) = Y_c(0)(1+\varepsilon), \qquad (6)$$

for the sensitivity-to-initial condition run, and except the parameter r,

$$r_b = r_c(1+\varepsilon), \qquad (7)$$

for the sensitivity-to-boundary condition run. Here, ε is a small error, and subscripts *i* and *b* represent the two sensitivity runs.

Introducing a same small relative error $\varepsilon = 0.0001$ to eitherthe initial or boundary condition, the Lorenz system has error growing and oscillation periods. For the parameter *r*, this error is equivalent to 0.01°C of the lower boundary temperature, 10% of the instrumentation accuracy for surface temperature measurement (Chu, 1999). Comparison of model output between the control run and the two sensitivity runs shows error growing and error oscillating stages (Fig. 1). During the growing period, the relative model error (i.e., error versus model internal variability) in both cases increases from 0 to an evident value larger than 1. During the oscillation period, the model error oscillates between two evident values. The model error growth is stronger and the growing period is shorter in the second kind (boundary condition error) than in the first kind (initial condition error).

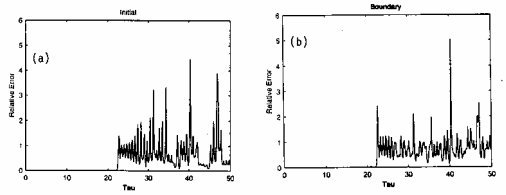

Figure 1. Model error evolution in the Lorenz system due to: (a) initial error, and (b) boundary error (from Chu 1999).

Is this phenomenon (predictability regarding boundary condition error) universal? What is the practical implication of the second kind unpredictability? We will use a recent version of the well-developed National Center for Atmospheric Research (NCAR) Community Climate Model Version 3 (CCM3) to test the existence of the second kind unpredictability. More precisely, we will investigate the atmospheric response to tiny and random disturbances of the sea surface temperature (SST). If the atmosphere is not sensitive to small random SST disturbances, we might consider nonexistence of the second kind predictability and use low resolution (in space and time) SST input to run atmospheric models. If the atmosphere is very sensitive to tiny and random SST disturbances, we must consider the second kind predictability and use high quality and high resolution SST data.

The outline of this paper is as follows. A model description and the experiment design are given in section 2. A depiction of the statistical test is given in section 3. The synoptic three-dimensional thermal structure and inverted velocity field is discussed in section 4. In section 5 we present our conclusions.

2. Numerical Experiment

2.1. Model Description

CCM3 has evolved from the Australian spectral model described by Bourke et al. (1977) and McAvaney et al. (1978). CCM3 is the most recent version of the NCAR Community Climate Model. It should be noted that CCM3 has a drastic change to the previous version, CCM2, especially due to the addition of the Biosphere-Atmosphere Transfer Scheme (BATS) documented in Dickinson et al. (1993). CCM3 still uses the spectral transform method for the dynamic equations but uses a semi-Lagrangian method for transporting water (Rasch and Williamson, 1991). The model we used here contains 18 levels in the vertical with a top at 2.917 mb, and uses spherical harmonics as horizontal basis functions with a

triangular truncation at wavenumber 21 (approximately a $5.6^o \times 5.6^o$ transform grid). The reader is referred to the foregoing articles for detailed description of the model physics (e.g., Kiehl 1990; Hack et al., 1993), apart from the radiative processes (e.g., Ramanathan et al., 1983; Briegleb, 1992; Slingo, 1989), atmospheric boundary layer processes (Troen and Mahrt, 1986; Holtslag et al., 1990), and mass flux scheme representing all types of moist convection (Hack, 1993).

2.2. Tiny Gaussian-Type SST Anomalies

We use a Gaussian-type random variable (δT) to represent SST anomalies. The probability distribution function is given by

$$F(\delta T) = \frac{1}{\sqrt{2\pi}} \exp\left[-\frac{(\delta T)^2}{2\sigma^2} \right], \qquad (8)$$

where δT is a random variable with a zero mean and a standard deviation of σ. Since our interest is to see the response of atmosphere to tiny random SST anomalies, we set

$$\sigma = 0.025^o \mathrm{C}$$

in this study. This value (0.025^oC) is much less than the current instrumentation error. If the atmosphere has a strong response to this tiny random SST error, we may conclude the existence of the second kind predictability problem.

2.3 Experiment Design

2.3.1. Control Run

The initial condition used in this study is 1 September's climatology of the atmospheric and surface fields, which was provided by the NCAR Climate and Global Dynamics (CGD) Division. The surface boundary conditions were monthly sea and land surface temperatures (also obtained from NCAR CGD Division) linearly interpolated onto each time step (20 min). We integrate CCM3 for ten months from 1 September to 30 June of the second year, and use the data between 1 January and 30 June of the second year for comparison.

2.3.2. Anomaly Run

After four months of the control run, we added a tiny Gaussian-type random SST anomaly with zero mean and 0.025^oC standard deviation generated by the FORTRAN random number generator applied to monthly SST data, and then interpolated into each time step. The rest of the forcing was kept the same. For the anomaly run, the model was integrated from the output of the control run on 1 January to 30 June of the second year (Fig. 2).

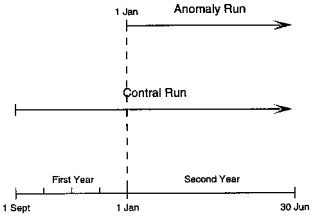

Figure 2. Control and anomaly runs.

We compare the model outputs such as surface level pressure, temperature, zonal and latitudinal velocities for 1 January to 30 June of the second year between the two runs, and call the difference between anomaly and control runs as the anomaly response.

3. Statistical Analysis

For a given vertical level, the anomaly response of any variable ψ is a function of space (x, y), and time t. We computed the standard deviation of the model output from the control run as the model internal variability and the root-mean-squares error (RMSE) between the control and the anomaly runs as the model anomaly response to the SST disturbance. The model internal variability of the variable ψ is depicted by its standard deviation of the model output for the control run,

$$SDV_\psi(t) = \sqrt{\frac{1}{M-1} \sum_i \sum_j \left[\psi_c(x_i, y_j, t) - \overline{\psi}_c(t) \right]^2} \qquad (9)$$

where M is the total number of horizontal grid points, the subscript 'c' indicates the control run, and $\overline{\psi}_c$ is the horizontal mean of ψ.

RMSE is defined by,

$$RMSE_{\psi}(t) = \sqrt{\frac{1}{M-1}\sum_i\sum_j\left[\psi_a(x_i,y_j,t)-\psi_c(x_i,y_j,t)\right]^2} \quad (10)$$

where the subscript *a* denotes the anomaly run. The ratio between RMSE and SDV,

$$E_{\psi}(t) = \frac{RMSE_{\psi}(t)}{SDV_{\psi}(t)}, \quad (11)$$

is the model relative error due to the tiny random SST disturbances.

4. Model Error Input

To detect the error propagation from SST to the atmosphere, we should first compute the relative SST error, $E_{SST}(t)$. The internal variability of surface temperature that is the standard deviation of the NCAR monthly sea and land surface temperatures is around 11.7°C. The root-mean-squares error of SST, $RMSE_{SST}(t) = 0.025$°C, is a constant throughout the experiment. The relative SST error, $E_{SST}(t)$, is 2×10^{-3} throughout the experiment.

5. Model Error Output

To investigate the error propagation and amplification from SST to the atmospheric models, we should compute the relative error. The larger the $E_{\psi}(t)$, the more uncertainty of the model due to the boundary condition (SST) error, and the more evident the existence of second kind unpredictability.

5.1. Surface Level Pressure (SLP)

The internal variability of the *SLP* field fluctuates between 80 mb and 87 mb (Fig. 3a). The RMSE of the *SLP* increases almost linearly from 0 to 14.2 mb within the 30 days (rapid growing period), and oscillates between 8 mb and 15 mb afterwards (Fig. 3b). The relative *SLP* error, $E_{SLP}(t)$, increases from 0 to 0.18 during the growing period, and oscillates between 0.10 and 0.18 during the oscillatory period after 30 days Fig.3c).

5.2. Temperature

The internal temperature variability has a little change with height: $SDV_T(t)$ varies between 14.2°-17.5°C at 850 mb (Fig. 4a), between 13.7°-15.5°C at 500 mb (Fig. 4b), and between 9.7°-14°C at 100 mb (Fig. 4c). The relative temperature error, $E_T(t)$, increases rapidly from 0 to noticeable values within 30 days at all heights: 0.48 at 850 mb (Fig. 4d), 0.37 at 500 mb (Fig. 4e), and 0.33 at 100 mb (Fig. 4f).

5.3. Zonal Wind

The internal variability of zonal winds increases with height: $SDV_U(t)$ varies between 6.5 - 8.2 m/s at 850 mb (Fig. 5a), between 8.7 - 11.6 m/s at 500 mb (Fig. 5b), and between 9.1-16.5 m/s at 100 mb (Fig. 5c). The relative zonal wind error, $E_U(t)$, increases rapidly from 0 to noticeable values within 30 days at all heights: 1.26 at 850 mb (Fig. 5d), 1.18 at 500 mb (Fig. 5e), and 0.9 at 100 mb (Fig. 5f).

5.4. Latitudinal Wind

The internal variability of latitudinal winds increases with height: $SDV_V(t)$ varies between 5.0 - 7.0 m/s at 850 mb (Fig. 6a), between 6.7 -9.8 m/s at 500 mb (Fig. 6b), and between 5.5-9.5 m/s at 100 mb (Fig. 6c). The relative zonal wind error, $E_V(t)$, increases rapidly from 0 to noticeable values within 30 days at all heights: 1.35 at 850 mb (Fig. 6d), 1.30 at 500 mb (Fig. 6e), and 1.38 at 100 mb (Fig. 6f).

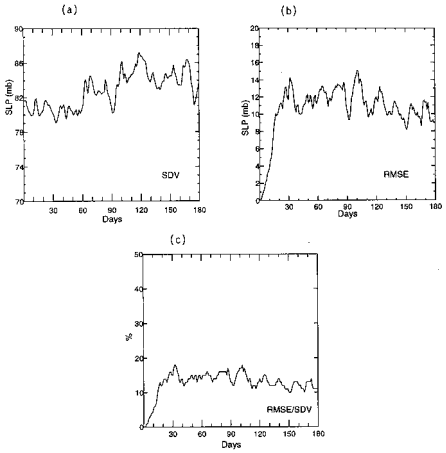

Figure 3. Response of sea level pressure to tiny SST errors: (a) internal variability (mb), (b) RMS error (mb), and (c) relative error.

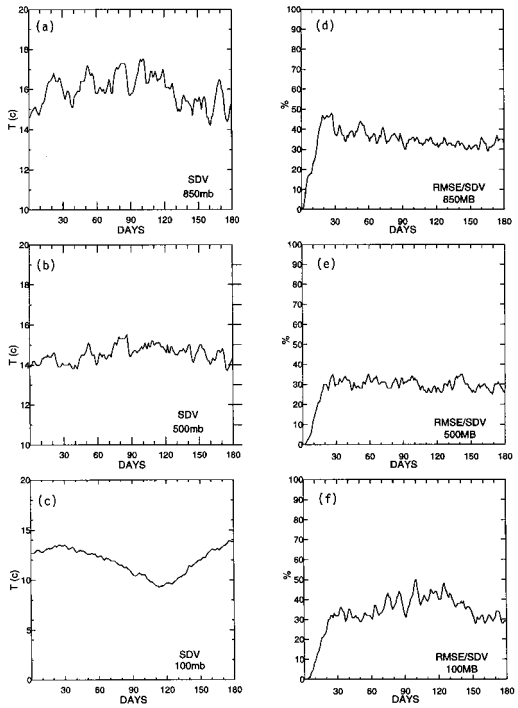

Figure 4. Response of air temperature to tiny *SST* errors: internal variability (^{o}C) at (a) 850 mb, (b) 500 mb, (c) 100 mb), and relative error at (d) 850 mb, (e) 500 mb, (f) 100 mb.

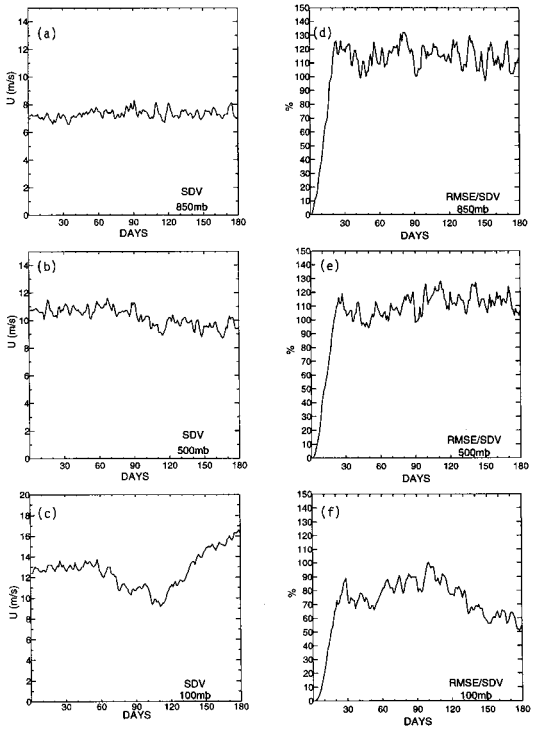

Figure 5. Response of zonal wind to tiny *SST* errors: internal variability (m/s) at (a) 850 mb, (b) 500 mb, (c) 100 mb), and relative error at (d) 850 mb, (e) 500 mb, (f) 100 mb.

6. Conclusions

(1) The second kind unpredictability is confirmed in this study using the NCAR CCM3. The climate model is sensitive to boundary condition error. Introducing a small relative SST error (0.002), the atmosphere has a growing period (0 to 30 day) and an oscillation period (after 30 days). During the growing period, the model error is amplified several hundred times as the error input from SST. During the oscillation period, the model error oscillates between two evident values.

(2) The global atmospheric response to a tiny random SST error (zero mean and 0.025^{o}C standard deviation) is quite strong. For example,

at 850 mb the RMS error of the zonal velocity is 1.35 time of the internal variability. This will lead to almost 10 m/s error.

(3) We estimate that the global atmospheric uncertainty comparing to the internal variability is around 0.3 to 0.5 for temperature, 0.9 to 1.3 for zonal wind, and 1.3 to 1.4 for latitudinal wind.

(4) Integration of an atmospheric model needs accurate SST data. The noise in the SST data may bring drastic change in the model results.

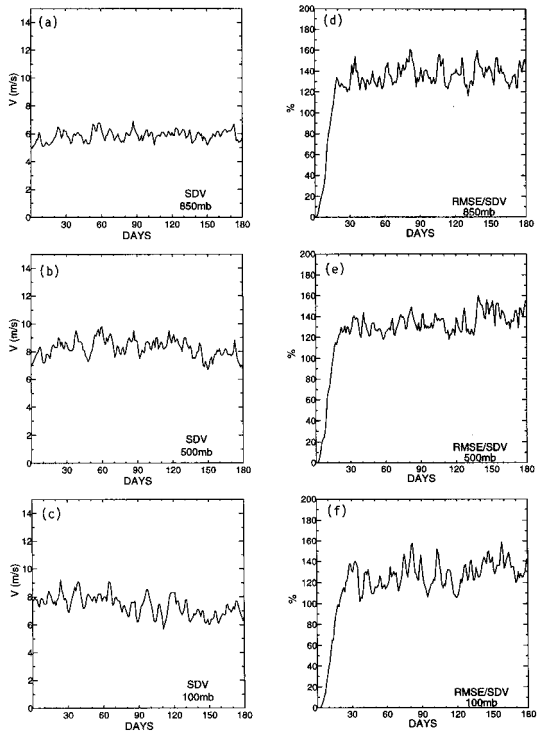

Figure 6. Response of latitudinal wind to tiny *SST* errors: (a) internal variability (m/s) at (a) 850 mb, (b) 500 mb, (c) 100 mb), and relative error at (d) 850 mb, (e) 500 mb, (f) 100 mb.

References

Bourke, W., B. McAvanney, K. Puri, and R. Thurling, 1977: Global modeling of atmospheric flow by spectral methods. Methods in Computational Physics, 17, General Circulation Models of the Atmosphere, J. Chang, Ed., Academic Press, 267-324.

Briegleb, B.D., 1992: Delta-Eddington approximation for solar radiation in the NCAR Community Climate Model. J. Geophys. Res., 97, 7603-7612.

Chu, P. C., 1999: Two kinds of predictability in the Lorenz system. J. Atmos. Sci., 56, 1427-1432.

Dickinson R.E., A. Herderson-Sellers, and P.J. Kennedy, 1993: Biosphere-Atmosphere Transfer Scheme (BATS) Version 1e as coupled to the NCAR Community Climate Model, *NCAR Technical Note*.

Hack, J.J., B.A. Boville, B.P. Briegleb, J.T. Kiehl, P.J. Rasch, and D.L. Williamson, 1993: Description of the NCAR Community Climate Model (CCM2), *NCAR Technical Note*, NCAR/TN-382+STR.

Holtslag, E.I., F. de Bruijn, and H.-L. Pan, 1990: A high resolution air mass transformation model for short-range weather forecasting. Mon. Wea. Rev., 118, 1561-1575.

Kiehl, J.T., Modeling and validation of clouds and radiation in the NCAR Community Climate Model. Proc. ECMWF/WCRP Workshop on Clouds, Radiative Transfer and Hydrological Cycle, 413-450, Reading, 12-15 November 1990.

Kutzbach, J.E., R.M. Chervin and D.D. Houghton, 1977: Response of the NCAR general circulation model to prescribed changes in ocean surface temperature Part I: Mid-latitude changes, J. Atmos. Sci., 34, 1200-1213.

Lorenz, E.N., 1963: Deterministic nonperiodic flow. J. Atmos. Sci., 20, 130-141.

McAvaney, B.J., W. Bourke and K. Puri, 1978: A global spectral model for simulation of the general circulation. J. Atmos. Sci., 35, 1557-1583.

Ramanathan, V., E.J. Pitcher, R.C., Malone and M.L. Blackmon, 1983: The response of a spectral general circulation model to refinements in radiative processes. J. Atmos. Sci., 40, 605-630.

Rasch, P.J. and D.L. Williamson, 1991: The sensitivity of a general circulation model climate to the moisture transport formulation. J. Geophys. Res., 96, 13,123-13,137.